Inverse Calculation of Composite Kink-Band Toughness from Open-Hole Compression Strength

Luke Borkowski and Rajesh S. Kumar[*]

United Technologies Research Center, 411 Silver Lane, East Hartford, CT 06108, USA

Abstract: Fiber-reinforced polymer matrix composite materials can fail by kink-band propagation mechanism when subjected to in-plane compressive loading. This mode of failure is especially prevalent in compressive loading of laminates with holes, cut-outs, or impact damage. Most of the successful models for predicting compressive strength of such laminates require "fracture" toughness associated with kink-band propagation under in-plane compression. However, this property is difficult to measure experimentally, limiting the use of such models in design practice. In this paper an inverse method is proposed to estimate the kink-band toughness of the laminate from its open-hole compression strength data, which is an easier property to measure experimentally. Furthermore, a scaling relationship is proposed to estimate kink-band toughness for other laminate configurations of the same material.

Keywords: A. Polymer Matrix Composites (PMCs); B. Strength, compression; B. Fracture toughness; C. Analytical modeling; Kink-band propagation

---
[*] Corresponding Author; Email: kumarRS@utrc.utc.com; Tel.: (860) 610-7045; Fax: (860) 353-2928

1. Introduction

Compression after impact (CAI) strength of composite laminates is one of the key properties required for initial sizing and design of composite structures for aerospace applications. This property is usually determined experimentally by subjecting laminates of interest to expected and/or required impact scenarios followed by in-plane compression testing. These experiments have been standardized by ASTM D7137 [ASTM D7137, 2012] so that the properties are measured in a consistent and repeatable manner. However, these tests are time consuming and expensive due to the wide range of parameters involved, especially for impact testing. For example, possible combinations of impactor mass, geometry, size, and velocity can create a large test matrix. Furthermore, as both the impact damage and the resulting CAI strength are a function of the laminate configuration (ply material and layup), testing is usually conducted on a narrow range of laminates based on past design experience. This limits the design space, especially during the preliminary design phase, to only those limited laminate configurations.

The limitations discussed in the foregoing paragraph have motivated the development of analytical and computational methods to predict impact damage [Dobyns, 1981; Cairns and Lagace, 1992, Abrate, 1994; Olsson, 2001; Esrail and Kassapoglou, 2014a] and CAI strength [Chen et al., 1993; Sekine et al., 2000; Habib, 2001; Yan et al., 2010; Nilsson et al., 2001; Hawyes et al., 2001; Xiong et al., 1995; Dost et al., 1988; Soutis and Curtis, 1996; Esrail and Kassapoglou, 2014b; Rhead and Butler, 2009] of polymer-matrix composite materials. CAI failure is a compression failure of the laminate that is weakened by the impact damage. There are two predominant failure mechanisms that can occur in CAI failure. These include local sublaminate buckling of the delaminated plies and kink-band initiation and propagation from the vicinity of the impact damage. The predominant mechanism can be different depending on the extent and the nature of the impact damage, material properties, and/or laminate configuration. It is also possible that the two mechanisms occur in a coupled manner where sublaminate buckling triggers the formation of the kink band that results in the final failure or vice versa. Based on these two mechanisms, there are two classes of analytical models proposed in the literature, namely, sublaminate buckling with or without delamination propagation [Shivakumar and Whitcomb, 1985; Chai and Babcock, 1985; Flanagan, 1988; Peck and Springer, 1991] and kink-band propagation models [Soutis and Curtis, 1996; Ratcliffe et al., 2004].

The models that are based on the kink-band propagation mechanism are also useful in predicting compressive failure of laminates with cut-outs such as open holes and notches as well as for CAI failure of sandwich panels [Soutis and Fleck, 1990; Soutis and Curtis, 1996; Ratcliffe et al., 2004]. However, kink-band propagation

models require measurement of kink-band toughness which is also referred to as compressive fracture toughness in literature. Kink-band toughness (represented by K_{Ic} throughout this manuscript) accounts for the initiation and propagation of the kink band and is related to the associated energy dissipation under compression. Implicitly, kink-band toughness accounts for the energy dissipation due to the underlying micro-mechanisms such as fiber micro-buckling and inelastic shear deformation in the matrix. However, kink-band toughness is not an easy property to measure and hence it is not readily available. To obtain this parameter, Soutis and co-workers [Soutis and Fleck, 1990; Soutis et al., 1991] employed a center-notched compression experiment while Ratcliffe et al. [2004] and Jackson and Ratcliffe [2004] used a compact compression test. A review and analysis of compressive fracture toughness testing methods in laminated composites is provided in Pinho et al. [2006]. Despite the effort in developing experimental techniques to characterize the kink-band toughness and in proving their effectiveness in doing so, currently there is no accepted standard procedure to measure this property. The difficulty in its measurement and lack of familiarity with the necessary testing methods limits the usefulness of kink-band-based CAI models, especially in an industrial design setting. While there have been attempts to determine the kink-band toughness from micromechanics-based models [Budiansky, 1983; Budiansky and Fleck, 1994; Jelf and Fleck, 1992; Soutis and Curtis, 2000], these models still require certain parameters that are not easily measured (e.g., shear yield strength of the laminate) or interpreted (e.g., fiber waviness angle). The present paper attempts to remedy this situation by estimating kink-band toughness from other readily available test data using an inverse methodology. The proposed methodology uses, as input, the unnotched compressive and open-hole compressive (OHC) strength properties, which can be measured using standardized test procedures (e.g., ASTM D6641 [2016] and ASTM D6484 [2014], respectively), to infer the kink-band toughness of the laminate. In addition, we demonstrate that the toughness scales with certain laminate elastic properties thus allowing prediction of kink-band toughness for other laminate configurations of the same material. The paper is organized as follows: in Section 2 we present the proposed inverse modeling approach. In Section 3 we demonstrate the procedure using OHC data available in literature and also develop the scaling relationships between the kink-band toughness and laminate attributes.

2. Approach

The inverse methodology proposed in this paper is based on the assumption that the open-hole compressive failure of PMC laminates occurs by kink-band initiation and propagation. This failure mechanism is likely to occur

for most structural PMC layups and hole diameters of interest, as has been shown in various previous works (see, for example, [Guynn and Bradley, 1989; Soutis et al., 1991; Soutis et al., 1993]). As kink-band propagation has been found to be the predominant mechanism in OHC failure of PMC laminates, attempts have been made to predict the OHC strength by modeling the kink-band initiation and propagation from the stress concentration regions of the open hole [Soutis et al., 1991; Soutis et al, 1993]. These "forward" analytical approaches require two key laminate-level properties – the unnotched compressive strength (σ_{unc}) and kink-band toughness (K_{Ic}). While the unnotched compressive strength can be easily obtained through standard experimental characterization or via calculations using, for example, laminate theory with an appropriate failure criterion, greater difficulty exists in quantifying the kink-band toughness. Thus, these models typically use K_{Ic} estimated from micromechanics models [Budiansky, 1983; Budiansky and Fleck, 1994; Jelf and Fleck, 1992; Soutis and Curtis, 2000] or, in some cases, measured from experiments [Soutis and Fleck, 1990; Soutis et al., 1991; Ratcliffe et al. [2004]; Jackson and Ratcliffe [2004]; Pinho et al., 2006].

As discussed in Section 1, CAI failure of composite structures also involves kink-band initiation and propagation and hence associated analytical models also require K_{Ic}. The commonality of this failure mechanism between OHC and CAI [Soutis and Curtis, 1996; Edgren et al., 2004; Hawyes et al., 2001; Ratcliffe et al., 2004] has motivated us to estimate K_{Ic} using the readily available OHC strength data via an inverse modeling approach. Once the K_{Ic} is estimated, it can be used in kink-band-based CAI strength prediction models. By requiring OHC strength data as input to the CAI models instead of K_{Ic} (which will be implicit and computed by the proposed inverse method), it is our expectation that the CAI strength prediction model will become more accessible to analysts and design engineers, especially during the preliminary design and sizing of composite structures.

2.1 Inverse Kink-Band Analysis

As previously described, one of the initial applications of the kink-band propagation model was for OHC strength prediction as a function of hole size, unnotched compressive strength, and kink-band propagation toughness [Soutis and Fleck, 1990; Soutis et al., 1991]. Hence, this method can be inverted so that it may provide the K_{Ic} value given the OHC strength, hole size, and unnotched compressive strength. We use the kink-band propagation models developed by Soutis and Fleck [1990] and Ratcliffe et al. [2004] in our inverse methodology. The basic equations for the kink-band analysis are discussed below for completeness.

Calculation of the OHC strength is conducted assuming the kink-band initiation and propagation mechanism consists of two competing growth stages – 1) stable kink-band growth governed by the stress concentration near the hole and the unnotched compressive strength of the laminate and 2) unstable kink-band propagation governed by the stress intensity factor at the kink-band tip and the fracture toughness of the laminate. The transition between stable and unstable growth determines the compressive strength, as shown schematically in Figure 1. Both cases assume symmetric kink-band propagation with respect to the centerline of the open hole, i.e., two kink bands propagate symmetrically from the two highest stress concentration points of the hole.

For stable kink-band growth, the average stress criterion of Whitney and Nuismer [1974] is used. In this criterion, stable kink-band growth is predicted to occur when the average stress over the kink band equals that of the unnotched laminate compressive strength, σ_{un}, i.e.,

$$\frac{r}{l} \int_{\xi=1}^{1+l/r} \sigma_y(\xi) d\xi = \sigma_{un} \tag{1}$$

where r is the hole radius, l is the kink-band length, σ_y is the stress in loading direction near the hole, and $\xi \equiv (r+l)/r$. The stress field in the vicinity of the hole, σ_y, can be approximated using the solution given by Konish and Whitney [1975] for an infinite orthotropic plate containing an open hole and loaded with a far-field stress, σ_s^{∞}, as

$$\sigma_y = \sigma_s^{\infty}\left[1 + \frac{1}{2}\xi^{-2} + \frac{3}{2}\xi^{-4} - \frac{(K_T - 3)}{2}\left(5\xi^{-6} - 7\xi^{-8}\right)\right] \tag{2}$$

where

$$K_T = 1 + \sqrt{\frac{2}{A_{22}}\left(\sqrt{A_{11}A_{22}} - A_{12} + \frac{A_{11}A_{22} - A_{12}^2}{2A_{66}}\right)} \tag{3}$$

is the stress concentration factor at the hole boundary for an orthotropic, symmetric, and balanced laminate plate [Konish and Whitney, 1975] where A_{ij} are elements of the laminate elastic stiffness matrix (see, for example, [Jones 1975]). It should be noted that the Konish and Whitney [1975] K_T approximation for an orthotropic plate is derived from the Lekhnitskii [1963] analytical expression for the stress in the loading direction near an open hole in an anisotropic plate. Substituting Eq. (2) into Eq. (1), the maximum average stress criterion can be stated as:

$$\sigma_s^\infty = \frac{\sigma_{un}}{m_{ave}} \tag{4}$$

where

$$m_{ave} = \frac{1}{\eta}\left[(1+\eta) - \frac{1}{2}(1+\eta)^{-1} - \frac{1}{2}(1+\eta)^{-3} + \frac{K_T - 3}{2}\left\{(1+\eta)^{-5} - (1+\eta)^{-7}\right\}\right] \tag{5}$$

and

$$\eta \equiv \frac{l}{r}. \tag{6}$$

Now using Eq. (4) , the far-field compressive stress leading to stable kink-band growth can be computed as a function of the kink-band length, as shown schematically by the stable kink-band growth curve in Figure 1.

For unstable propagation of the kink band, a linear elastic fracture mechanics approach is employed where unstable kink-band growth is assumed to occur when the stress intensity factor at the kink-band tip exceeds the compressive "fracture" toughness of the material [Paris and Sih, 1965], giving:

$$\sigma_u^\infty = \frac{K_{Ic}}{\sqrt{\pi\eta r}\, f_h f_w} \tag{7}$$

where σ_u^∞ is the far-field stress for unstable growth, K_{Ic} is the compressive kink-band toughness of the laminate, and f_h and f_w are geometrical factors, expressed as

$$f_h = 1 - 0.15\lambda + 3.46\lambda^2 - 4.47\lambda^3 + 3.52\lambda^4 \tag{8}$$

with

$$\lambda = (1+\eta)^{-1} \tag{9}$$

and

$$f_w = \sqrt{\sec\left(\frac{\pi r}{w}\right)\sec\left(\frac{\pi(r+l)}{w}\right)}. \tag{10}$$

The expression for the geometric factor, f_h, presented in Eq. (8) is a polynomial fit by Newman [1976] of the complex variable solution by Bowie [1956] that accounts for the effect of the stress concentration due to the hole on the stress intensity factor at the crack tip. A finite width geometric factor, f_w, accounts for the effect of the

specimen edge, i.e., finite width, on the stress state near the hole and crack tip [Newman, 1976]. Further details of the mathematical formulation governing kink-band formation and growth can be gathered from Soutis and Fleck [1990], Soutis et al. [1991], Soutis and Curtis [1996], and Ratcliffe et al. [2004].

To calculate the OHC strength given the kink-band toughness and other parameters, i.e., "forward" analysis, the intersection of the curves defined by Eqs. (4) and (7) is sought for various virtual kink-band lengths. A root-finding procedure is employed to determine the solution of the following equation for a range of kink-band lengths:
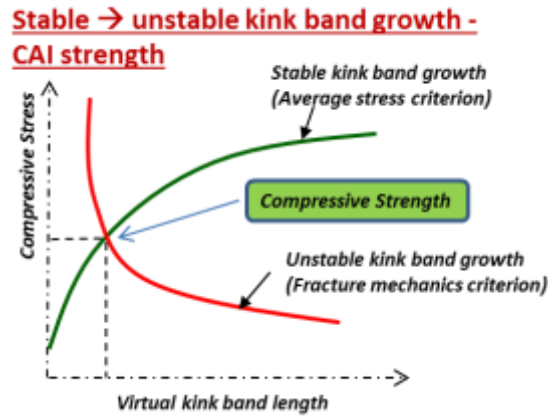
$$\sigma_s^{\infty} - \sigma_u^{\infty} = 0. \tag{11}$$

Figure 1. Kink-band growth criterion schematic

Now, in order to perform the inverse analysis required to compute K_{Ic} from σ_{OHC}, we utilize the fact that the kink-band propagation model predicts OHC strength when the curves for stable and unstable kink-band growth intersect as shown in Figure 1 (i.e., Eq. (4) and Eq. (7) are equal). Therefore at the point of compressive failure, $\sigma_{OHC} = \sigma_s^{\infty} = \sigma_u^{\infty}$. Knowing σ_s^{∞}, as well as the lamina elastic and laminate unnotched compressive strength, one can use Eq. (4) to solve for η. Utilizing this value of η, the hole radius, and the known value of σ_u^{∞}, Eq. (7) can then be used to solve for K_{Ic}. Based on the outlined procedure, available OHC data for any hole size and laminate configuration can be employed to calculate the desired values for K_{Ic} for that laminate.

In order to be useful, the calculated K_{Ic} should be independent of the hole size. It will be shown in the next section that this is indeed the case. However, it is important to note that the calculated K_{Ic} is a laminate level

property, i.e., it will be different for different laminate configurations. This is limiting as the calculated K_{Ic} can then be used only for the exact same laminate configuration. As discussed earlier, the intended use of the calculated K_{Ic} is for CAI impact analysis during design, especially during initial preliminary design phases where a range of laminate configurations might be explored. Therefore, in order to increase the generality, it would be useful to develop a methodology to predict kink-band toughness for other laminate configurations of the same material. In Section 3 we will show that the calculated K_{Ic} can be linearly scaled by laminate thickness, laminate stiffness (axial, combination of axial and shear), and unnotched compressive strength, with the combination of axial and shear stiffness based scaling providing the best correlation. With such scaling relationships developed for a particular material, kink-band toughness for any other laminate can be estimated and used in CAI strength prediction models.

3. Results and Discussion

Investigations were carried out to quantify the capability of the inverse analysis method outlined in Section 2 in predicting the kink-band propagation toughness from OHC strength data. One such investigation included an analysis of NASA OHC strength data provided in Hodge et al. [2011]. This dataset consists of OHC strength for six hole diameters in three different layups of IM7/8552-1 including one "hard" [45,0,-45,0,90,0,0,90,0]$_s$, one "soft" [-45,90,45,90,0,90,90,0,90]$_s$, and one "quasi-isotropic" [-45,90,45,0]$_{2s}$ layup (Figure 2). The goal of our analysis was to determine whether the K_{Ic} values predicted using the inverse method for each laminate were consistent (i.e., minimal variance) for multiple hole diameters. As described in Soutis and Fleck [1990], Hodge et al. [2011], and Jackson and Ratcliffe [2004], a low variance in the K_{Ic} data provides evidence that this parameter is material- and laminate-specific and not a function of the hole diameter. Therefore if K_{Ic} is independent of hole diameter, using data from an OHC strength test for a single hole size based on the ASTM standard testing procedure [ASTM D6484, 2014] in conjunction with the inverse analysis methodology discussed in the foregoing section, one could determine the necessary K_{Ic} value. Using the data shown in Figure 2 and applying the developed inverse methodology discussed in Section 2, a value for K_{Ic} for each σ_{OHC} data point was predicted. The results are shown in Figure 3 where the average K_{Ic} value for each hole diameter and layup is plotted (point markers) in addition to the overall mean K_{Ic} value for each laminate (lines). It is seen that the variability observed in the predicted K_{Ic} values is small and similar magnitude to the variability in experimental OHC strength data, which indicates that this parameter can in fact be considered a laminate-level material property. This is consistent with the conclusion reached by Soutis and

Fleck [1990]; Hodge et al. [2011]; and Jackson and Ratcliffe [2004]. One can also observe from Figure 3 that the value for K_{Ic} is strongly correlated with the laminate layup given the large difference in average kink-band propagation toughness values for the "hard", "quasi-isotropic", and "soft" layups of the same material system.
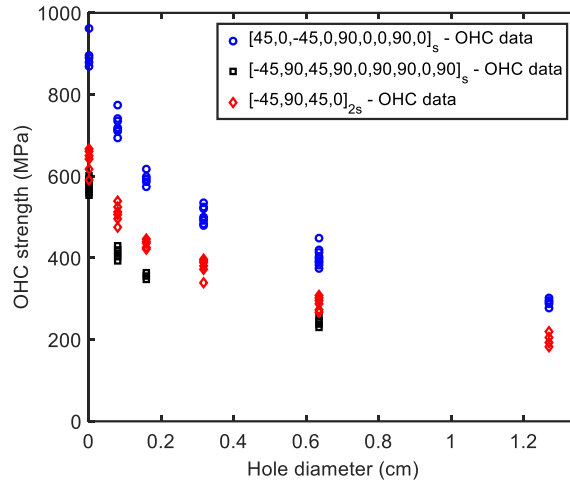

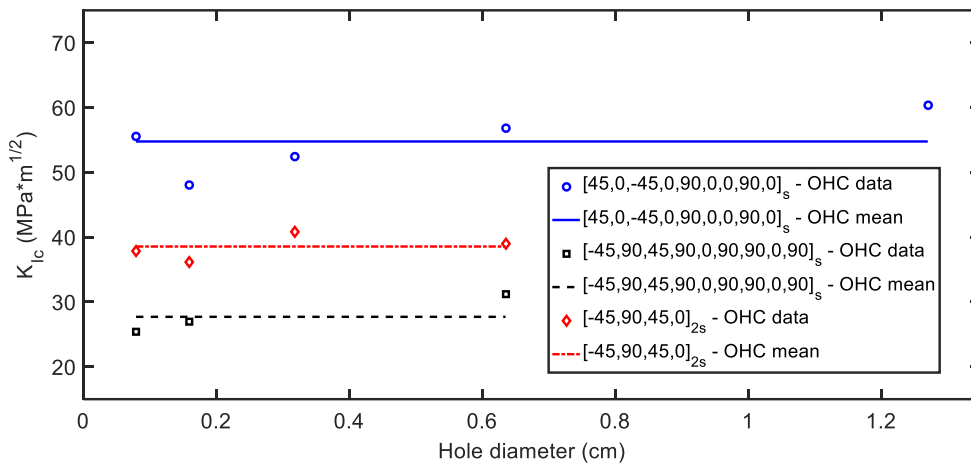Figure 2. OHC strength as a function of hole diameter [Hodge et al., 2011]

Figure 3. Kink-band propagation toughness, K_{Ic}, values predicted using OHC strength data

With the introduction of the proposed inverse analysis technique, four methods currently exist to obtain the value for K_{Ic}. These include 1) performing a non-standard compact compression or center-notched compression experiment [Soutis and Fleck, 1990; Soutis et al., 1991; Ratcliffe et al., 2004; Jackson and Ratcliffe, 2004; Pinho et al., 2006], 2) using a "typical" value from a sufficiently similar laminate, 3) estimating an approximate value using micromechanics [Budiansky, 1983; Budiansky and Fleck, 1994; Jelf and Fleck, 1992; Soutis and Curtis, 2000], and

9

4) computing the value from OHC strength data, using the inverse analysis method proposed in this paper. As mentioned in Section 1, the lack of a standard testing method for measuring K_{Ic} prevents its current widespread adoption. Additionally, Figure 3 illustrates how widely K_{Ic} can vary for different layups of the same composite material system, indicating that Method 2 has limited applicability. Method 3 has been used with some success for specific cases to estimate K_{Ic} and will be further evaluated later in this manuscript. Therefore of these four methods, computing K_{Ic} from OHC strength data seems to offer the best balance between generality and accuracy.

3.1. Scaling Relationship: Estimating Kink-Band Toughness for Other Layups

In order to provide even greater generality for OHC and CAI strength prediction models and to maximize the number of possible design considerations for rapid design frameworks utilizing these models, scaling relationships were investigated to determine if one could estimate K_{Ic} for laminate configurations other than those for which OHC strength data is available. For example, if a designer has access to test data (e.g., unnotched and open-hole compressive strength) for three separate laminates of the same material system, could an empirical relationship be determined that would then allow the designer to compute the CAI strength for laminate configurations for which no experimental characterization data exists? In order to answer this question, the K_{Ic} values predicted using the inverse analysis method were plotted against various elastic, strength, and layup properties to assess their correlation. Figure 4 shows the correlation between K_{Ic} values and the longitudinal elastic modulus (E_x), percentage of 0° plies, sum of longitudinal elastic modulus and in-plane shear modulus ($E_x + G_{xy}$), and unnotched compressive strength (σ_{un}). For this particular material system, the kink-band propagation toughness correlates best with the sum of the longitudinal elastic modulus and in-plane shear modulus ($E_x + G_{xy}$) with an R^2 value of >0.999. Since kink-band compressive failure involves both fiber micro-buckling and matrix inelastic shear, the excellent correlation observed between K_{Ic} and ($E_x + G_{xy}$) appears to be consistent with the physical mechanisms that lead to compressive failure in the case of OHC. As seen in Figure 5, normalizing the K_{Ic} data based on the laminate value for ($E_x + G_{xy}$) effectively collapses the three curves into one narrow band. Provided with this scaling relationship, a designer could determine K_{Ic} values for additional laminates without the needed for additional OHC strength test data.
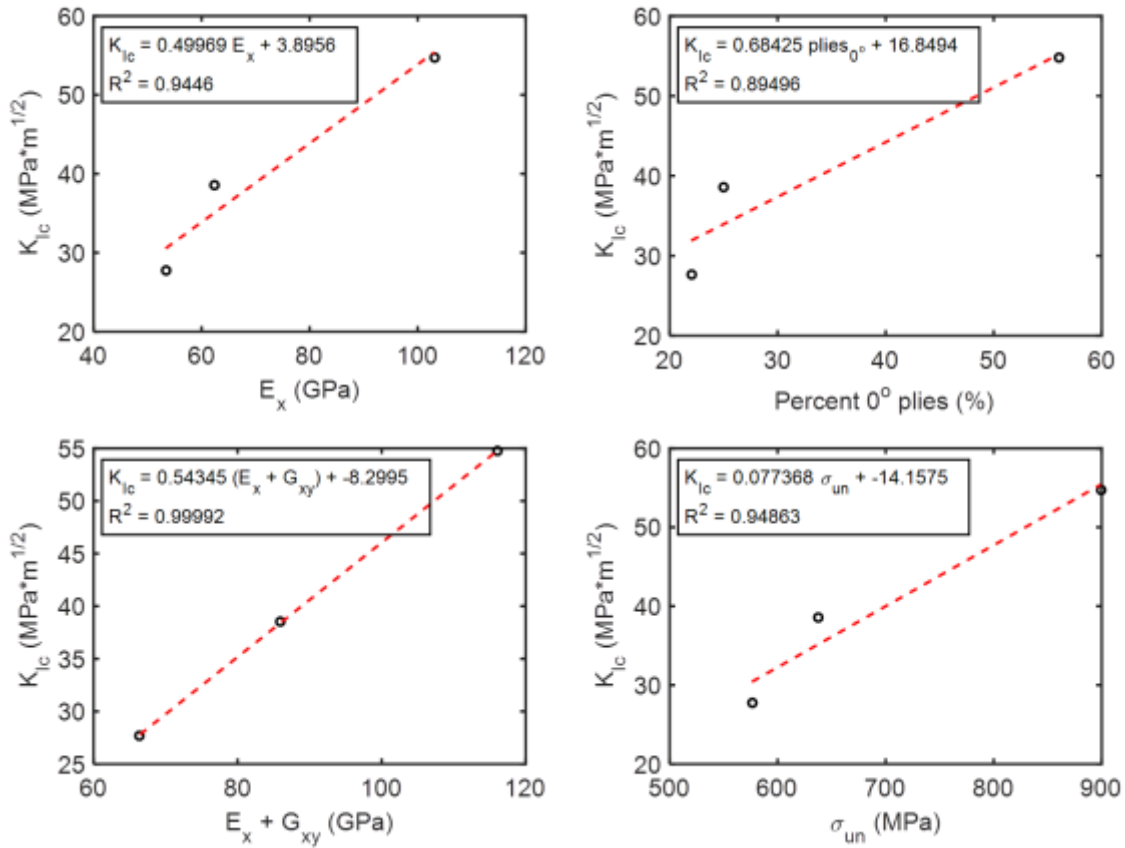
Figure 4. K_{Ic} scaling with respect to various elastic and strength parameters for three laminates of IM7/8552
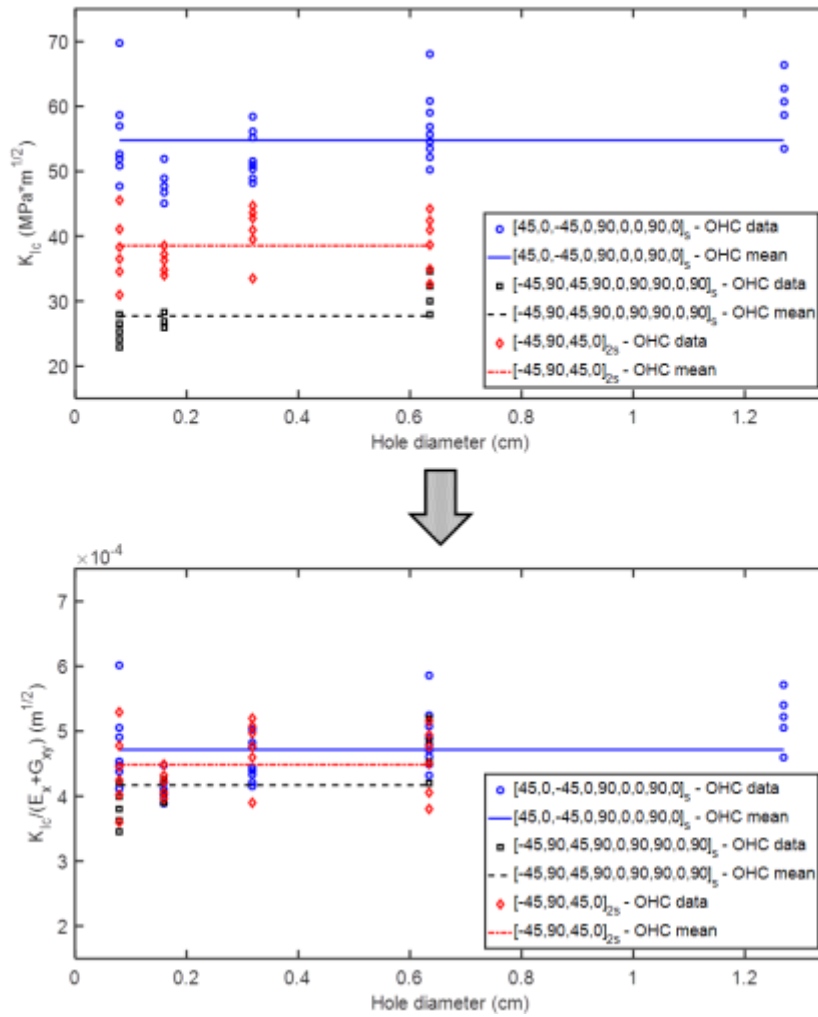
Figure 5. Effect of scaling/normalization based on $(E_x + G_{xy})$ – collapse of K_{Ic} vs. hole diameter data

It has been demonstrated that utilizing the scaling method based on $(E_x + G_{xy})$ can collapse predicted K_{Ic} data. This correlation can then be used to predict kink-band propagation toughness for other layups under investigation for OHC or CAI strength analysis but lack the necessary data to compute K_{Ic} using the inverse method outlined previously. While the band of data shown in Figure 5 is narrow, some variance still exists. Therefore an investigation was carried out to determine the effect of this observed deviation on the predicted CAI strength for two laminates and impact scenarios presented in literature. For the first case, presented in Sanchez-Saez [2005], the CAI strength was predicted for an AS4/3501-6 cross-ply laminate with an elliptical impact damage profile of size 2a=12.0 and 2b=8.0 mm. The CAI strength was also predicted for an impact scenario, presented in Lee et al. [2011], of an IM7/8552 quasi-isotropic laminate with a circular impact damage diameter of 17.0 mm. To predict the CAI

strength governed by kink-band initiation and propagation, the model presented in Section 2 was utilized and a value

of K_{Ic} = 40.0 MPa*m$^{1/2}$ [Soutis and Curtis, 1996] was specified for both CAI strength prediction modeling cases.

The prediction error for the experimental CAI strength presented in Sanchez-Saez [2005] and Lee et al. [2011] were

approximately 0.1% and 7%, respectively. Now, in order to assess the error one could incur if the scaling

relationship based on in-plane elastic properties is used to collapse the data presented in Figure 5, CAI strength

prediction simulations of the Sanchez-Saez [2005] and Lee et al. [2011] laminates and impact scenarios were carried

out for a range of K_{Ic} values. Based on the standard deviation of the mean normalized K_{Ic} values presented in Figure

5, a ±2σ range (35.11 – 44.89 MPa-m$^{1/2}$) is highlighted in red vertical dashed lines in Figure 6. It should be noted

that this ±2σ range is smaller than the range of typical K_{Ic} values presented in literature (35 – 50 MPa-m$^{1/2}$ [Soutis

and Curtis, 1996]). As observed in Figure 6, the CAI strength prediction error is small (<11% for the Lee et al.

[2011] data and <8% for the Sanchez-Saez [2005] data) for the prescribed ±2σ range of K_{Ic}. These results provide

confidence in the accuracy of CAI strength results predicted using K_{Ic} values determined from scaling relationships

based on laminate elastic properties and fit using the developed inverse analysis technique.
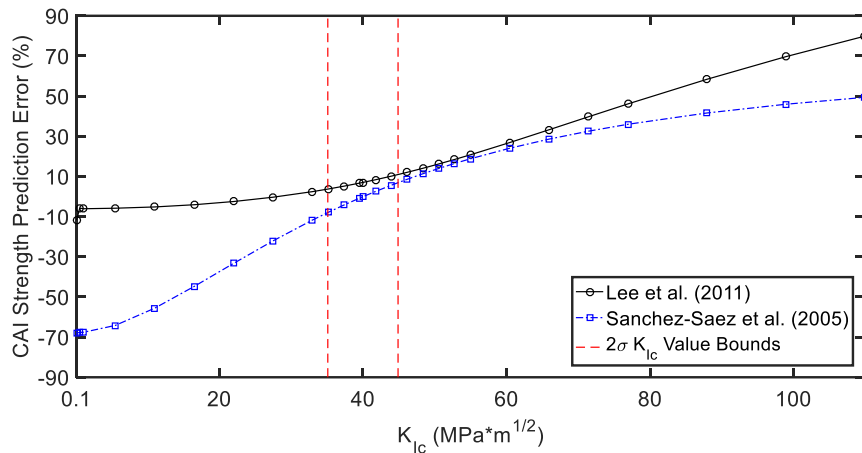

Figure 6. Sensitivity of CAI strength prediction with respect to K_{Ic} value

Based on the observation that the predicted K_{Ic} values can be considered a laminate-level property (i.e.,

function of laminate material system, layup, and processing parameters) and the success in determining a scaling

method for K_{Ic} as a function of in-plane elastic properties of the laminate, an investigation was carried out on an

additional composite material system commonly utilized in aerospace composite structures, AS4/8552. The primary

intent of analyzing AS4/8552 using the inverse method and complimentary scaling approach was to determine if this

framework could be accurately applied to different material systems. Experimental data from Marlett et al. [2011a]

including laminate OHC and unnotched compressive strength and lamina elastic properties were used in the inverse analysis to estimate the kink-band toughness (K_{Ic}) from OHC strength. Again, three different laminates were considered including one "hard" [0/45/0/90/0/-45/0/45/0/-45]$_s$, one "soft" [45/-45/0/45/-45/90/45/-45/45/-45]$_s$, and one "quasi-isotropic" [45/0/-45/90]$_{2s}$. The OHC strengths for the three laminates [Marlett et al., 2011a] are plotted in Figure 7. After computing the values of kink-band toughness for each of the OHC strengths, the effectiveness of correlating K_{Ic} to various elastic and strength parameters was assessed as was done for IM7/8552 (Figure 4). The linear fits for K_{Ic} vs E_x, percent 0° plies, ($E_x + G_{xy}$), and σ_{un} are presented in Figure 8 in addition to their respective linear equations and coefficients of determination (R^2). Similar to IM7/8552, the sum of in-plane extension and shear moduli provided the best correlation with kink-band propagation toughness, resulting in an R^2 value of approximately 0.979. The second-best correlation parameter for both IM7/8552 and AS4/8552 is the unnotched compressive strength (σ_{un}). However, since in-plane elastic properties of the laminate can be accurately computed from the lamina elastic properties using classical lamination theory (CLT), scaling K_{Ic} based on ($E_x + G_{xy}$) will provide the greatest generality as well as accuracy.
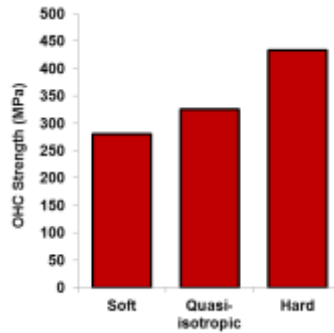

Figure 7. OHC strength data for three layups of AS4/8552 [Marlett et al., 2011a]
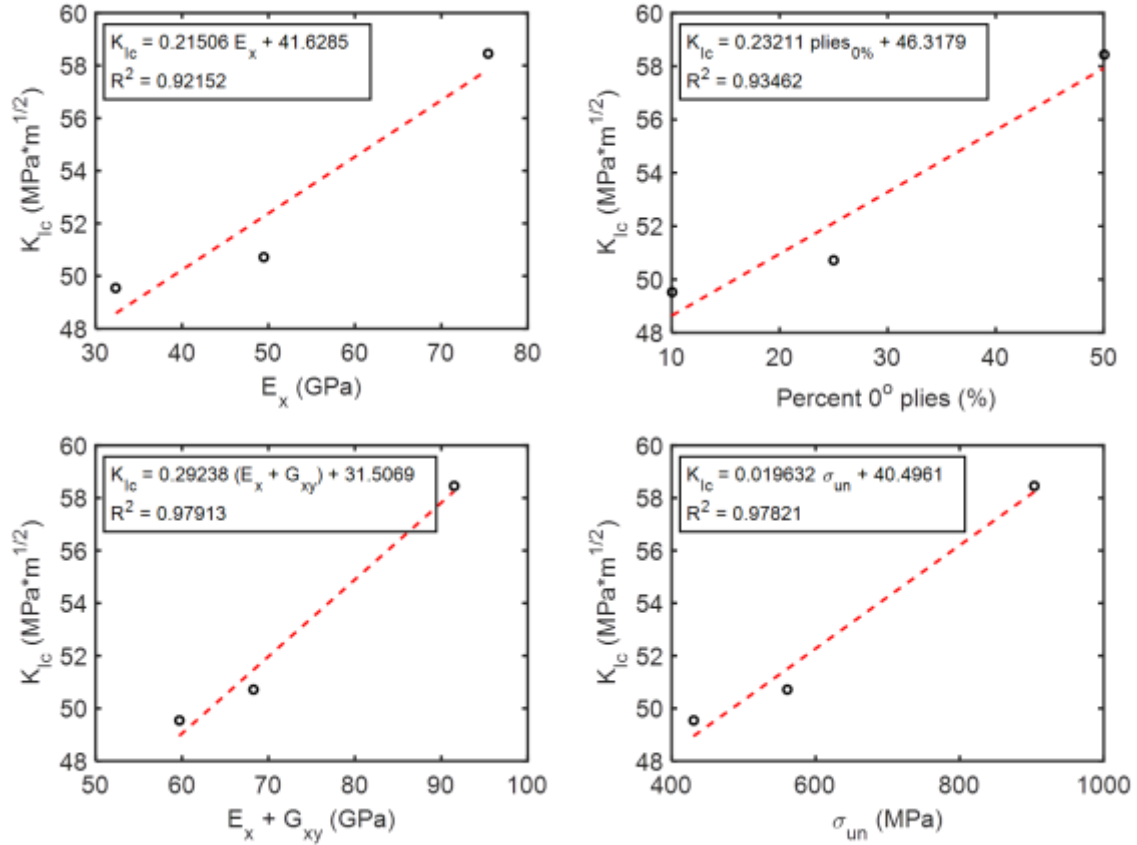
Figure 8. K_{Ic} scaling with respect to various elastic and strength parameters for three laminates of AS4/8552

3.2. Remarks on the Micromechanics Approach

Since it is often the case that experimental data for K_{Ic} via compact compression or center-notched compression experiments is not available for a specific laminate / material system combination of interest, micromechanics is often called upon to obtain the necessary value in order to simulate kink-band initiation and propagation from an open hole or impact damage [Soutis and Curtis, 2000]. One such micromechanics model by Budiansky [1983] is presented in Eq. (12)

$$w = 2v_c = \frac{\pi d_f}{4}\left(\frac{V_f E_f}{2\tau_y}\right)^{1/3} \tag{12}$$

where w is the kink-band width, v_c is the critical crack closing displacement (CCD), d_f is the fiber diameter, V_f is the fiber volume fraction, E_f is the fiber Young's modulus, and τ_y is the laminate in-plane shear yield strength.

The Mode I critical strain energy release rate, G_{Ic}, can be computed as a function of the critical crack closing displacement, v_c, and the laminate unnotched compressive strength, σ_{un}, using Eq. (13).

$$G_{Ic} = 2\int_0^v \sigma(v)dv = \sigma_{un}v_c \tag{13}$$

Finally, the kink-band propagation toughness, K_{Ic}, for an orthotropic plate under plane stress conditions containing a crack parallel to a plane of symmetry is calculated using Eq. (14) [Kanninen and Popelar, 1985] where a_{ij} are elements of the elastic compliance matrix where $\varepsilon_i = a_{ij}\sigma_j$, $j = 1,\cdots,6$.

$$G_{Ic} = K_{Ic}^2 \left(\frac{a_{11}a_{22}}{2}\right)^{1/2} \left[\left(\frac{a_{22}}{a_{11}}\right)^{1/2} + \frac{2a_{12} + a_{66}}{2a_{11}}\right]^{1/2} \tag{14}$$

In addition, an empirical relation obtained by Jelf and Fleck [1992] through fitting of a function of similar form as Eq. (12) to various composite data found in literature, presented in Eq. (15), can be used to compute the kink-band width.

$$w = 0.68d_f \left(\frac{V_f E_f}{\tau_y}\right)^{0.37} \tag{15}$$

Eqs. (12) through (15) were called upon to provide estimates of K_{Ic} for three layups of IM7/8552 (Laminate 1: [45/0/-45/90]$_{3s}$, Laminate 2: [45/-45/0/45/-45/90/45/-45/45/-45]$_s$, and Laminate 3: [0/45/0/90/0/-45/0/45/0/-45]$_s$). The required elastic and strength parameters for the micromechanics models were obtained from Marlett et al. [2011b] and Hexcel [2016] datasheet. K_{Ic} values for each of the three laminates using the Budiansky [1983] (Eq. (12)) and the Jelf and Fleck [1992] (Eq. (15)) models are shown in Table 1. The predicted values for K_{Ic} using both models are low compared with the range of values typically observed for carbon fiber reinforced polymer matrix composites. In order to assess the effect of the micromechanics-based estimates of K_{Ic} values on the predicted OHC strength, the values in Table 1 were used to compute the OHC strength using the model presented in Section 2. The experimental [Marlett et al., 2011b] and predicted OHC strength values are presented in Table 2 with the percent error shown in parentheses. It can be observed that using micromechanics to compute the K_{Ic} value results in an underprediction of the OHC strength. The average errors over the three laminates for the Budiansky [1983] and Jelf and Fleck [1992] models are 27.84% and 21.35%, respectively.

Table 1. Predicted K_{Ic} values using the Budiansky [1983] and Jelf and Fleck [1992] micromechanics models

		Laminate 1	Laminate 2	Laminate 3
K_{Ic} (MPa*m$^{1/2}$)	Budiansky	28.95	23.88	29.16
	Jelf & Fleck	35.04	28.9	35.29

Table 2. Predicted OHC strength (σ_{OHC}) using the micromechanics-based K_{Ic} values shown in Table 1; comparison (error in parentheses) with experimental values from Marlett et al. [2011b]

		Laminate 1	Laminate 2	Laminate 3
σ_{OHC} (MPa)	Experiment	338.39 (-)	267.52 (-)	436.02 (-)
	Budiansky	250.00 (26.12%)	204.43 (23.58%)	288.61 (33.81%)
	Jelf & Fleck	274.48 (18.89%)	221.53 (17.19%)	314.13 (27.96%)

4. Conclusions

Motivated by the goal of improving the applicability of OHC and CAI simulation methods based on kink-band propagation failure mechanisms, an inverse methodology was developed to estimate kink-band toughness (K_{Ic}) using OHC data. Direct measurement of K_{Ic} has been demonstrated to be feasible [Soutis and Fleck, 1990; Jackson and Ratcliffe, 2004] however it requires using non-standard test methods such as compact or center-notched compression tests. Researchers and practitioners wanting to utilize validated OHC or CAI models requiring this parameter [Soutis and Fleck, 1990; Soutis et al., 1991; Soutis and Curtis, 1996; Ratcliffe et al., 2004] have previously had to rely on "typical" values for sufficiently similar laminates or have called upon micromechanics to provide estimates of the values. The presented inverse approach now provides an additional method for estimating this necessary parameter. Results indicate that the approach is capable of predicting K_{Ic} for a wide range of laminate layups for two polymer matrix composite systems commonly used in aerospace applications (IM7/8552 and AS4/8552). Furthermore, it was shown that the approach can be generalized to predict the K_{Ic} for other layups using simple linear scaling relationships. An investigation was carried out assessing the possible error resulting from using a scaling procedure based on the sum of the in-plane extension and shear moduli of the laminate. It was found that for a $\pm 2\sigma$ variation in K_{Ic} (standard deviation determined from scaled K_{Ic} data), a maximum error of 11% could be expected. In the initial design stage for a composite structure, this magnitude of error is typically acceptable. The

accuracy of two micromechanics-based methods of approximating K_{Ic} were also investigated and found to produce errors over 20% in most cases for OHC strength prediction. It is envisioned that the proposed inverse methodology will reduce the barrier for adoption of kink-band-based rapid analysis tools for CAI strength prediction, especially during the preliminary design of composite structures.

Acknowledgements:

References:

Abrate S. Impact on laminated composites: recent advances. Appl Mech Rev 1994;47(11):517-544.

ASTM D6484 / D6484M-14. Standard Test Method for Open-Hole Compressive Strength of Polymer Matrix Composite Laminates. ASTM International; 2014.

ASTM D6641 / D6641M-16. Standard Test Method for Compressive Properties of Polymer Matrix Composite Materials Using a Combined Loading Compression (CLC) Test Fixture. ASTM International; 2016.

ASTM D7137 / D7137M-12. Standard Test Method for Compressive Residual Strength Properties of Damaged Polymer Matrix Composite Plates. ASTM International; 2012.

Bowie OL. Analysis of an infinite plate containing radial cracks originating at the boundary of an internal circular hole. Stud in Appl Math 1956;35(1-4):60-71.

Budiansky B. Micromechanics. Comput Struct 1983;16(1-4):3-12.

Budiansky B, Fleck NA. Compressive kinking of fiber composites: A topical review. Appl Mech Rev 1994;47(6):S246-S270.

Cairns DS, Lagace PA. A consistent engineering methodology for the treatment of impact in composite materials. J Reinf Plast Compos 1992;11(4):395-412.

Chai H, Babcock CD. Two-dimensional modelling of compressive failure in delaminated laminates. J Compos Mater 1985;19(1):67-98.

Chen VL, Wu HYT, Yeh HY. A parametric study of residual strength and stiffness for impact damaged composites. Compos Struct 1993;25(1):267-275.

Dobyns AL. Analysis of simply-supported orthotropic plates subject to static and dynamic loads. AIAA J 1981;19(5):642-650.

Dost EF, Ilcewicz LB, Gosse JH. Sublaminate Stability Based Modeling of Impact-Damaged Composite Laminates. In: Proceedings of the American Society for Composites: Third Technical Conference: Integrated Composites Technology 1988. p. 354-363.

Edgren F, Asp LE, Bull PH. Compressive failure of impacted NCF composite sandwich panels-Characterisation of the failure process. J Compos Mater 2004;38(6):495-514.

Esrail F, Kassapoglou C. An efficient approach for damage quantification in quasi-isotropic composite laminates under low speed impact. Composites Part B 2014;61:116-126.

Esrail F, Kassapoglou C. An efficient approach to determine compression after impact strength of quasi-isotropic composite laminates. Compos Sci Technol 2014;98:28-35.

Flanagan G. Two-dimensional delamination growth in composite laminates under compression loading. In: Composite Materials: Testing and Design (Eighth Conference) January, 1988. ASTM International; 1988.

Guynn EG, Bradley WL. A detailed investigation of the micromechanisms of compressive failure in open hole composite laminates. J Compos Mater 1989;23(5):479-504.

Habib FA. A new method for evaluating the residual compression strength of composites after impact. Compos Struct 2001;53(3):309-316.

Hawyes VJ, Curtis PT, Soutis C. Effect of impact damage on the compressive response of composite laminates. Composites Part A 2001;32(9):1263-1270.

Hexcel. HexTow Carbon Fiber Product Data Sheet. http://www.hexcel.com/resources/datasheets/carbon-fiber-data-sheets/im7.pdf; 2016.

Hodge AJ, Nettles AT, Jackson JR. Comparison of Open-Hole Compression Strength and Compression After Impact Strength on Carbon Fiber/Epoxy Laminates for the Ares I Composite Interstage. NASA/TP—2011–216460; 2011.

Jackson WC, Ratcliffe JG. Measurement of fracture energy for kink-band growth in sandwich specimens. Composites testing and model identification. Composites testing and model identification 2004:21-23.

Jelf PM, Fleck NA. Compression failure mechanisms in unidirectional composites. J Compos Mater 1992;26(18):2706-2726.

Jones RM. Mechanics of composite materials. Scripta Book Company; 1975

Kanninen MF, Popelar CL. Advanced fracture mechanics. Oxford Engineering Science Series; 1985.

Konish HJ, Whitney JM. Approximate stresses in an orthotropic plate containing a circular hole. J Compos Mater 1975;9(2):157-166.

Lee J, Soutis C, Kong C. Prediction of compression-after-impact (CAI) strength of CFRP laminated composites. In: ICCM International Conferences on Composite Materials. August, 2011.

Lekhnitskii SG. Of an anisotropic elastic body. San Francisco: Holden-Day; 1963.

Marlett K, Ng Y, Tomblin J. Hexcel 8552 AS4 unidirectional prepreg 190 gsm & 35% RC qualification material property data report. National Center for Advanced Materials Performance, Wichita, Kansas. Test Report CAM-RP-2010-002, Rev. A; 2011:1-278.

Marlett K, Ng Y, Tomblin J. Hexcel 8552 IM7 unidirectional prepreg 190 gsm & 35% RC qualification material property data report. National Center for Advanced Materials Performance, Wichita, Kansas. Test Report CAM-RP-2009-015, Rev. A; 2011:1-238.

Nilsson KF, Asp LE, Alpman JE, Nystedt L. Delamination buckling and growth for delaminations at different depths in a slender composite panel. Int J Solids Struct 2001;38(17):3039-3071.

Newman Jr JC. Predicting failure of specimens with either surface cracks or corner cracks at holes. NASA TN D-8244; 1976.

Olsson R. Analytical prediction of large mass impact damage in composite laminates. Composites Part A 2001;32(9):1207-1215.

Paris PC, Sih GC. Stress analysis of cracks. In: Fracture toughness testing and its applications. ASTM International; 1965.

Peck SO, Springer GS. The behavior of delaminations in composite plates—Analytical and experimental results. J Compos Mater 1991;25(7):907-929.

Pinho ST, Robinson P, Iannucci L. Fracture toughness of the tensile and compressive fibre failure modes in laminated composites. Compos Sci Technol 2006;66(13):2069-2079.

Ratcliffe J, Jackson WC, Schaff J. Compression strength prediction of impact-damaged composite sandwich panels. In: Proceedings of the American Helicopter Society: 60th Annual Forum June, 2004, Baltimore, MD; 2004.

Rhead AT, Butler R. Compressive static strength model for impact damaged laminates. Compos Sci Technol 2009;69(14):2301-2307.

Sánchez-Sáez S, Barbero E, Zaera R, Navarro C. Compression after impact of thin composite laminates. Compos Sci Technol, 2005;65(13):1911-1919.

Sekine H, Hu N, Kouchakzadeh MA. Buckling analysis of elliptically delaminated composite laminates with consideration of partial closure of delamination. J Compos Mater 2000;34(7):551-574.

Shivakumar KN, Whitcomb JD. Buckling of a sublaminate in a quasi-isotropic composite laminate. J Compos Mater 1985;19(1):2-18.

Soutis C, Fleck NA. Static compression failure of carbon fibre T800/924C composite plate with a single hole. J Compos Mater 1990;24(5):536-558.

Soutis C, Fleck NA, Smith PA. Failure prediction technique for compression loaded carbon fibre-epoxy laminate with open holes. J Compos Mater 1991;25(11):1476-1498.

Soutis C, Curtis PT, Fleck NA. Compressive failure of notched carbon fibre composites. In: Proceedings of the Royal Society of London A: Mathematical, Physical and Engineering Sciences February, 1993;440(1909):241-256.

Soutis C, Curtis PT. Prediction of the post-impact compressive strength of CFRP laminated composites. Compos Sci Technol 1996;56(6):677-684.

Soutis C, Curtis PT. A method for predicting the fracture toughness of CFRP laminates failing by fibre microbuckling. Composites Part A 2000;31(7):733-740.

Whitney JM, Nuismer RJ. Stress fracture criteria for laminated composites containing stress concentrations. J Compos Mater 1974;8(3):253-265.

Xiong Y, Poon C, Straznicky PV, Vietinghoff H. A prediction method for the compressive strength of impact damaged composite laminates. Compos Struct 1995;30(4):357-367.

Yan H, Oskay C, Krishnan A, Xu LR. Compression-after-impact response of woven fiber-reinforced composites. Compos Sci Technol 2010;70(14):2128-2136.